Available online at www.sciencedirect.com

ScienceDirect

Advances in Space Research 54 (2014) 435–442

ADVANCES IN SPACE RESEARCH (a COSPAR publication)

www.elsevier.com/locate/asr

Occurrence of equatorial plasma bubbles over Kolhapur

A.K. Sharma [a], D.P. Nade [a,*], S.S. Nikte [a], P.T. Patil [b], R.N. Ghodpage [b], R.S. Vhatkar [a], M.V. Rokade [a], S. Gurubaran [c]

[a] *Earth and Space Science Laboratory, Department of Physics, Shivaji University, Kolhapur 416004, India*
[b] *Medium Frequency Radar, Indian Institute of Geomagnetism, Kolhapur 416004, India*
[c] *Indian Institute of Geomagnetism, New Panvel, Navi Mumbai 410218, India*

Available online 22 July 2013

Abstract

This paper reports the nightglow observations of OI 630.0 nm emissions, made by using all sky imager operating at low latitude station Kolhapur (16.8°N, 74.2°E and dip lat. 10.6°N) during high sunspot number years of 24th solar cycle. The images are analyzed to study the nocturnal, seasonal and solar activity dependence occurrence of plasma bubbles. We observed EPBs in images regularly during a limited period 19:30 to 02:30 LT and reach maximum probability of occurrence at 22:30 LT. The observation pattern of EPBs shows nearly no occurrence during the month of May and it maximizes during the period October–April. The equinox and solstice seasonal variations in the occurrence of plasma bubbles show nearly equal and large differences, respectively, between years of 2010–11 and 2011–12.

Keywords: Plasma bubbles; All sky imager; OI 630.0 nm images; Equinox; Solstice

1. Introduction

In F region, at low latitude, the plasma irregularities have been frequently observed. Due to these irregularities regions of large scale ionospheric depletions of electron density (as compared to the background ionospheric plasma density) are developed, which are called "equatorial plasma bubble (EPB)". The ionospheric dynamics, at low latitudes, is closely related to EPBs which are the region of reduction of ions along the magnetic field lines (Weber et al., 1978). Generally, the plasma bubbles are generated in the bottom side of F-region (e.g. Abalde et al., 2004). The EPB is believed to be generated, at the equator, mainly by the non-linear evolution of the Generalized Rayleigh–Taylor (GRT) instability (Shvarts et al., 1996), E × B drift instabilities (e.g. Kelley et al., 2011) and growth of strong gravity-waves (Taori et al., 2010) as well as other instabilities reported by Taori et al. (2013). The gravity waves play an important role in temporal separation of plume occurrence (Taori et al., 2011) and seeding EPBs by RT instability (Taori et al., 2012). These EPBs move up to maximum altitude and go down on low latitude region at both sides of the equator.

Based on numerous studies using satellite and ground data, it is widely accepted that the nightglow OI 630.0 nm emissions are generated at low latitude F-region heights (250–300 km) (Pimenta et al., 2001b). The variations of F-region height were studied by Sahai et al. (2004a) during most of the storm period. Therefore OI 630.0 nm emissions are very important to study the EPBs at low latitude region. In OI 630.0 nm image the dark bands or intensity depleted regions are the signatures of EPBs. This phenomenon and its signature have been studied from Kolhapur using photometers (Mukherjee and Shetti, 2008; Jagtap et al., 2010; Jagtap and Sharma, 2008), and all-sky imaging system (Mukherjee et al., 2000; Parihar et al., 2012). Several investigators have used all sky imaging system (OI 630.0 nm emission) to study the onset, evolution and dynamics of EPBs (e.g. Weber et al.,

* Corresponding author. Tel.: +91 2312609349.
E-mail address: dada.nade@gmail.com (D.P. Nade).

0273-1177/$36.00 © 2013 COSPAR. Published by Elsevier Ltd. All rights reserved.
http://dx.doi.org/10.1016/j.asr.2013.07.018

1980; Sahai et al., 1994; Taylor, 1997; Mukherjee et al., 1998; Fagundes et al., 1999; Sinha et al., 2001). In the Brazilian sector, Pimenta et al. (2008) presented the occurrence of dark band structures in the OI 630 nm nightglow emission all-sky images during different solar activity conditions. It is of scientific interest to study the occurrence of EPBs because they cause random error and cause scintillations for the satellite signals which results in problems in communication and navigation system.

The F-region nightglow emission at (^{1}D) IO 630.0 nm, are governed by dissociative recombination between O_2^+ and electrons (Dashora et al., 2012). The reaction mechanism are given below

$O_2^+ + e \rightarrow O + O^*$ (Mukherjee et al., 2000; Sharma et al., 2012)

Here superscript on oxygen indicates the excited state; these excited atoms (oxygen) radiate the 630.0 nm emissions,

$O^* \rightarrow O + h\upsilon_{(630\ \mathrm{nm})}$ (Mukherjee, 2006; Sharma et al., 2012).

2. Instrumentation and observations

Regular observations of nightglow OI 630.0 nm were carried out during clear, moonless nights from low latitude station Kolhapur (16.8°N, 74.2°E and dip lat. 10.6°N). This is a scientific collaborative program between Shivaji University, Kolhapur and Indian Institute of Geomagnetism (I.I.G.), Navi Mumbai. A high resolution (1024 × 1024 pixels) CCD (13.3 × 13.3 mm to 27.6 × 27.6 mm), back-illuminated array with a pixel depth of 16 bits based all sky imager (ASI) is used to measure the nightglow OI 630.0 nm emission from Kolhapur. The quantum efficiencies of the ASI are >95%. Low dark current (0.5 electrons/pixel/s) with low readout noise and high linearity of ASI useful to achieve quantitative observation of the nightglow emissions. The fish eye lens (f/4 Mamiya RB67) having focal length 24 mm and tele-centric lens system are used to collect the signal from the atmosphere. The images in OI 630.0 nm, OI 557.7 nm, 840.0 nm, 846.0 nm, and OH Meinel bands at 720.0–910.0 nm and the transmission of background light in 857.0 nm to be obtained with integration time of typically 120 s, 120 s, 06 s, 06 s, 90 s and 10 s, respectively. A more detailed discussion of this experimental setup is presented by Nade et al. (2012) and Sharma et al. (accepted for publication).

For this work, we have taken data of image in OI 630.0 nm for the period between October 2010 and May 2012 to study the percentage of occurrence of EPBs. Fig. 1 shows some of successive images in OI 630.0 nm, recorded on 19–20 May 2012 for the period between 21:32:21 LT and 21:54:39 LT (Local Time = Universal Time + 05:30) by all sky imager from Kolhapur (16.42°N, 74.2°E, and 10.6°N dip lat.). In Fig. 1, all images show clear sky (without features). For more identification of EPBs, we have processed all the images using “averaging” method. The averaging method involves two steps. At first, averaging of one hour image data is done and then its subtraction from each image is obtained. This is necessary to take care of readout counts and hot pixels present in the observations (Taori et al., 2013). Fig. 2 illustrates some of the successive images having intensity depleted regions or the EPBs, obtained by all sky imager on 15–16 February 2012 for the period between 21:46:49 LT and 22:09:48 LT. In Fig. 2, the structures of EPBs are easily identifiable and small scale irregularities are also seen distinctly. In Fig. 2 the red[1] arrows indicate the motion of north–south aligned plasma bubble from west to east.

From the processed images, it is possible to identify the signature of EPBs. The ground based observations in OI 630.0 nm by all sky imager is a unique technique to study the evolution and dynamics of EPBs. Sahai et al. (2000) have presented the effect of solar cycle on the occurrence of EPBs, observed in OI 630.0 nm images from Cachoeira Paulista, Brazil. They reported that the frequency of occurrence of EPBs was high during the months of Octobers to March while it was very low during May to August in the Brazilian sector. Sahai et al. (1998) reported the occurrence of EPBs, highly correlated with geomagnetic disturbances, during the period of March 1987 to October 1991.

Data of radio flux at $F_{10.7\mathrm{cm}}$, proton flux and ΣK_P index (available at http://sec.noaa.gov) are used to study the effect of solar and geomagnetic activities on occurrence of EPBs. The ΣK_P (daily sum) index is a global average of geomagnetic activity, sampled at 3 h intervals in real time from magnetometers operating at mid-latitude stations. The $F_{10.7\mathrm{cm}}$ (2800 MHz) (full Sun radio flux) is reported by the Dominion Radio Astrophysical Observatory at Penticton, B.C., Canada on the dates indicated. Values are in solar flux units of $10^{-22}\ \mathrm{W\ m^{-2}\ Hz^{-1}}$. Measurements are made around 2000 UTC. The plot of proton flux contains integral proton flux (protons/cm s sr) averaged for five minutes as measured by the Space Whether prediction Center (SWPC) Primary GOES satellite, nearly 75° West, for each of the three energy thresholds: greater than 10, 50, and 100 MeV.

Here we have studied the occurrence of EPBs as a function of season, solar activity and magnetic activity. We give, first a short description of nightglow OI 630.0 nm observations and then compare our results with those from earlier studies.

3. Results and discussion

During the observation of the nightglow in OI 630.0 nm emission (for the period of two years), 5185 of images

[1] For interpretation of color in Figs. 2 and 4–7, the reader is referred to the web version of this article.

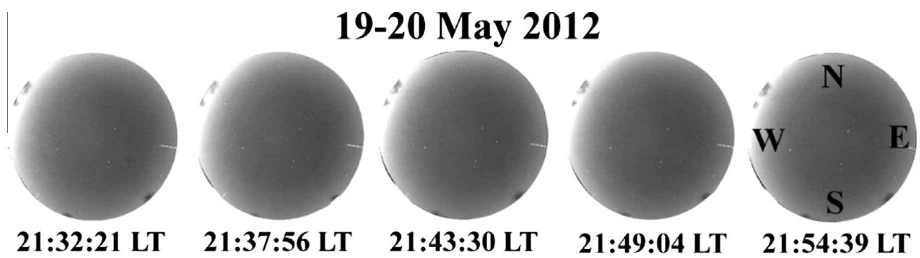

Fig. 1. Some of the successive images in OI 630.0 nm, without plasma bubbles, recorded by all sky imager on 19–20 May 2012 from low latitude station Kolhapur.

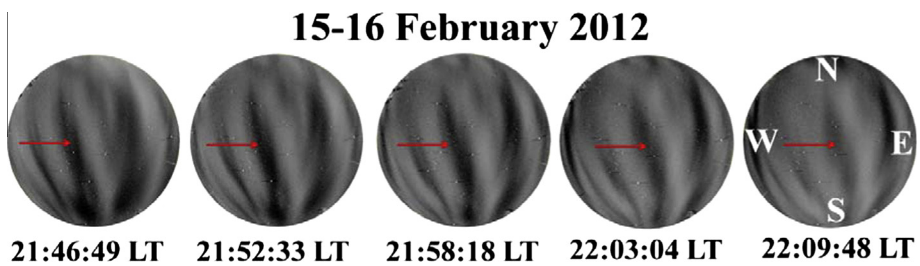

Fig. 2. Some of the processed successive images in OI 630.0 nm, with plasma bubbles, recorded by all sky imager on 15–16 February 2012 from low latitude station Kolhapur.

showed the presence of EPBs. They detected as “quasi” north–south aligned intensity depletions, very similar to that of presented and discussed by Mukherjee et al. (1998). The occurrence of EPBs varies on day-to-day basis. Fig. 3 shows the mean nocturnal variations in the occurrences of EPBs. The possibility of occurrence of EPBs increases rapidly after 19:30 LT and reaches maximum value at about 22:30 LT. Day-to-day occurrence of changes in peak value is indicated by standard deviations in the Fig. 3. The present results are very much similar to the nocturnal variations of EPBs occurrence reported by Sahai et al. (2000).

The seasonal patterns and longitudinal variations of equatorial spread-F have been studied by several investigators. The occurrence of seasonal variation of EPBs has

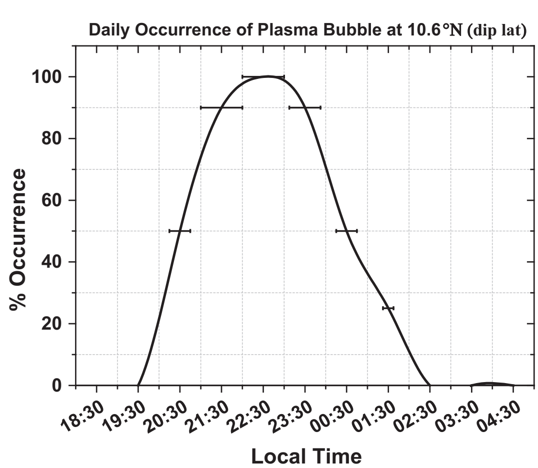

Fig. 3. Daily occurrence of plasma bubble over Kolhapur (10.6° dip lat.).

been studied, using the nightglow in OI 630.0 nm from Cachoeira Paulista, by Sahai et al. (1994). Lee et al. (2009), first time, reported the probabilities of occurrence of ionospheric irregularities using three different measurements: ionosonde, Global Positioning System (GPS) and satellite, during solar maximum year (2000). The nighttime variations are categorized into three seasons: Equinox (E) months (March, April, September and October), June solstice (J) months (May, June, July and August), and December solstice (D) months (January, February, November and December). Herein, we have shown the seasonal occurrence of EPBs using OI 630.0 nm obtained by the all sky imager at low-latitude station Kolhapur, India. In the Indian sector, the occurrence of F region irregularities has been studied by several researchers using ionosonde (Chandra et al., 2003), VHF/UHF/L band scintillations (DasGupta et al., 1981; Chakraborty et al., 1999), total electron content (TEC) (Dashora et al., 2012).

In Table 1, details of observations of OI 630.0 nm emissions for the period October–May of 2010 and 2012 are summarized. It is clear that from Table 1, the number of solar flux ($F_{10.7\mathrm{cm}}$) is lower during period of 2010–11 (94 ± 7) than 2011–12 (128 ± 22). Fig. 4 presents the night-to-night variations in the probabilities of occurrence of EPBs in equinoxes (E) periods of 2010–11 and 2011–2012. We defines the probability of occurrence as the number of images on which at least one EPB is observed in one night divided by the total number of images recorded on same night. In Fig. 4, blue bars indicate night time variations in the percentage occurrence in October 2010, March 2011 and April 2011 while red for October 2011, March 2012 and April 2012. Due to unsuitable (cloudy) climate we could not taken the observations of OI 630.0 nm images

Table 1
Shows the results of observations during period of solar activity.

Sr. no.	Descriptions	Period of 2010–2011	Period of 2011–2012
1	Average solar flux (F 10.7)	94 ± 7	128 ± 22
2	Total number of images (nights)	7808 (80)	10000 (103)
3	Number of images (nights) during equinox period (Oct., Mar. and Apr.)	2884 (33)	3070 (34)
4	Images [nights] with plasma bubble during equinox period	1150 (40%) [22 (66.67%)]	1169 (38%) [25 (73.53%)]
5	Number of images (nights) during solstice period (Nov. to Feb.)	3753 (39)	5774 (57)
6	Images [nights] with plasma bubble during solstice period	561 (15%) [17 (43.59%)]	2313 (40%) [49 (85.96%)]

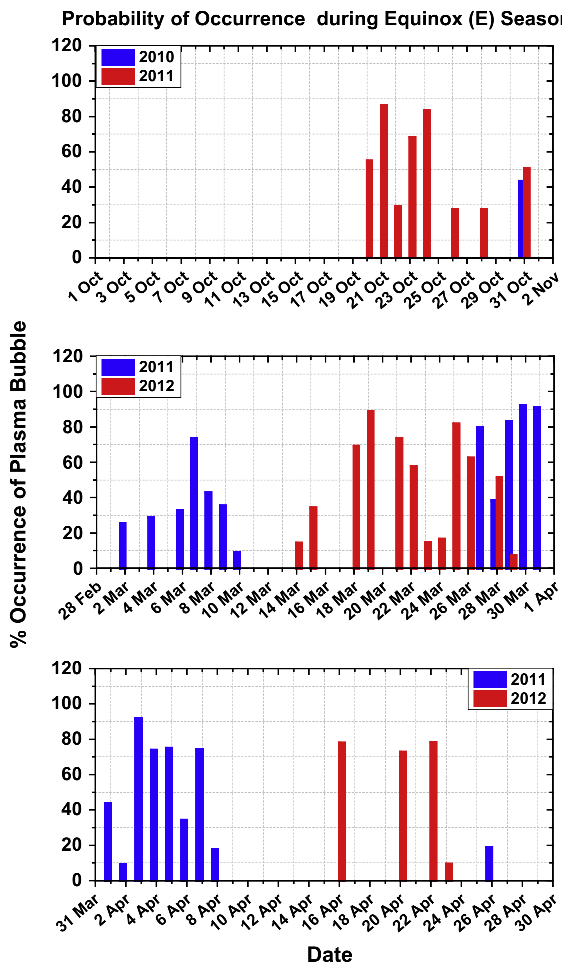

Fig. 4. The variation in percentage of occurrence of plasma bubble during equinox period – October, March and April.

during month of September. Therefore in Fig. 4, the month of September is not included. It is noted that the monthly averaged probabilities of occurrence are very low in October 2010 (10.08%) than that in October 2011 (61.86%) and March 2011 (22.25%) than in March 2012 (44.61%) while very high in April 2011 (61.86%) than in April 2012 (21.42%). However, overall probabilities of occurrence of EPBs are nearly same during equinox periods of 2010–11 (39.87%) and 2011–12 (38.08%).

Here we present the nights showing occurrence of EPBs in each month. These probabilities is calculated as the number of nights showing signature of EPBs divided by total number of nights in month. This occurrence is low in 2010 (25%) than in 2011 (100%) (months of October) while it was high in 2011 (69.23%) than 2012 (33.33%) (months of April). The nights of 2011 (75%) and 2012 (92.86) (months of March) show nearly same probabilities of occurrence. The average of probabilities of occurrence of EPBs in each months of equinox period was comparatively less in 2010–11 (66.67%) than that in 2011–12 (73.53%).

Fig. 5 shows the night-to-night variations in probabilities of occurrence of EPBs, in terms of image, during the December solstice (D) (i.e. November to February of 2010–11 and 2011–12). These probabilities are (14.94%) for 2010–11 and (40.05%) for 2011–12. The percentage of useful nights (for meaningful data) during November 2010 to February 2011 is about 43.59 while for November 2011 to February 2012 it is about 85.96. The total number of nights of observations, number of nights having EPBs and percentage of occurrence of EPBs for each month are summarized in Table 1.

The observations of number of nights during each season are summarized in Table 1. From Table 1 it is clear that very low probabilities of occurrence of EPBs in OI 630.0 nm images obtained in May months of 2011 and 2012. It also supports the findings of (Sahai et al., 1998 and 1999) indirectly as they reported absence of EPBs during the months of May–August. We could not record the data of imager from June to August due to unsuitable conditions for observations. It is noted that during May 2012, only one out of 12 nights showed the presence of EPBs. Sahai et al. (2000) have found this occurrence only on nights having magnetic disturbances during J months (May to August). The occurrence of EPB is very low during the period May, whereas it maximizes during October–March. These results are in agreement with that of reported by Sahai et al. (2000). Radar observations from Jicamarca, Peru have also reported that during the June solstice, the occurrence of radar plumes (which is equivalent to bubbles in optical measurements) is very low compared to equinox and December solstice (Chapagain et al., 2009). In Indian sector, the period of May is last month of local summer and starting of local rainy season. Therefore this is last month of observations of all sky imager. The nightglow observations in OI 630.0 nm from Kolhapur (10.6° dip lat.)

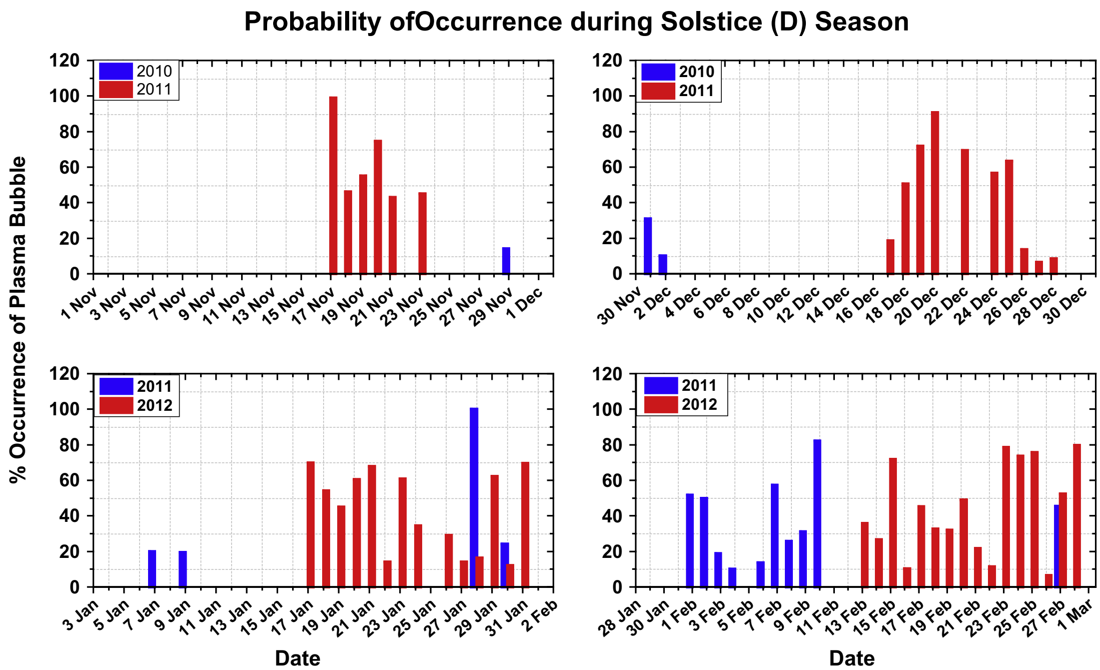

Fig. 5. The variation of percentage of occurrence of plasma bubble during Solstice season, November to February.

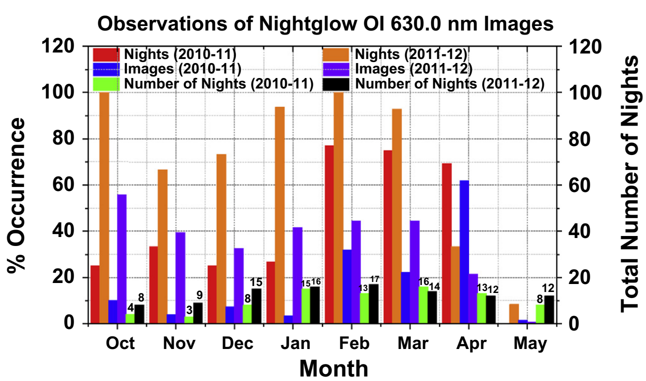

Fig. 6. The observation of nightglow in OI 630.0 nm over Kolhapur (10.6° dip lat.). The red and orange bars indicate the percentage of number of nights with events along with blue and violet bars indicate the percentage of number of event images observed and bars indicated by green and black shows the number of nights on which observations was made on each month of the period between October 2010 and May 2012. (For interpretation of the references to colour in this figure legend, the reader is referred to the web version of this article.)

are summarized in Fig 6. In this figure the probabilities of monthly occurrence of EPBs in nights are shown as red and orange bars for October 2010–May 2011 and October 2011–May 2012, respectively and images as blue and violet bars for October 2010–May 2011 and October 2011–May 2012, respectively. The green and black bars are shows the number of nights on which observations was made on each month of the period between October 2010 and May 2012.

The equatorial spread F and VLF scintillation occur most frequently during equinoxes and they are minimum in winter (Huang, 1970). However (Chandra et al., 2003) reported these to be moderate in winter and maximum in equinoxes when sunspots are maximum. The occurrence of the EPB is found to be maximum in the equinoxes and solstice during high sunspot year (2011–12). Sahai et al. (2004b) reported that the maximum occurrence of EPBs during the period October–March. Abdu et al. (1985) reported maximum occurrence of equatorial spread-F during October–March in the Brazilian sector.

From Fig. 7 it is clear that the probability of occurrence correlates with the values of $F_{10.7\mathrm{cm}}$ during the period of October to January of years 2010 and 2011, minimum (below 90) is indicated by a column in grey while maximum (above 120) during February–April 2011 is indicated by green column (Fig. 7(a)). Generally, solar wind-induced geomagnetic activity tends to suppress equatorial spread-F (Kelley et al., 2000). During solar maximum, occurrence of EPBs and bottom-side spread-F depend on season, magnetic activity and $E \times B$ drift velocity (Whalen, 2002). Fig. 7 shows that the probability of occurrence depends on solar activity. We found these to be more during period of high solar flux ($F_{10.7\mathrm{cm}}$), particle flux (>10 MeV) and ΣK_P index. So we can say that the probabilities depend on solar activity. It is also clear, from Fig. 7, that the occurrence of EPBs has a linear relationship with ΣK_P index. This result is in good agreement with that of Whalen (2002), he has shown that during equinoxes and solstice period EPBs increase with geomagnetic activity. Pimenta et al. (2001a) reported that the bifurcation occurrences of EPB were higher during high solar activity than low solar activity.

In this paper, we have presented the seasonal occurrence of EPBs during high sunspot activity year of 24th solar

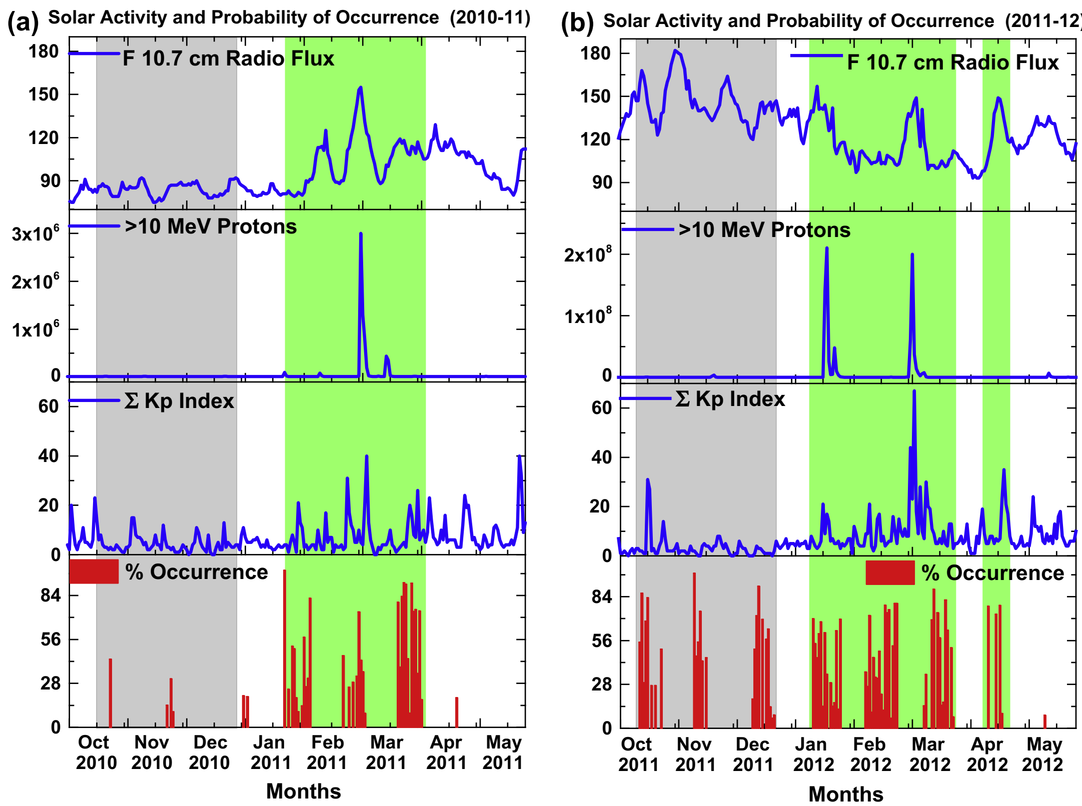

Fig. 7. The relation between solar activity and percentage of occurrence of plasma bubble during period between October 2010 and May 2012.

cycle, based on the number of images and nights with and without EPBs. At the dip equator, after sunset, plasma irregularities are generated in the bottom side of F region mainly because of the Rayleigh–Taylor (R-T) instability (e.g. Kelley, 1989). These plasma irregularities lift from magnetic equator to higher altitudes due to the equatorial plasma fountain effect (Lin et al., 2007) and then it diffuses down along the magnetic field lines to higher latitudes creating two ionization crests on both the sides of the magnetic equator. However the equatorial $E \times B$ upward drift reaches its maximum value during 22:00–23:00 LT (Scherliess and Fejer, 1997) and consequently plasma fountain effect occurs. Hence probability of occurrence of EPBs, at low latitude region, maximize during 22:00–23:00 LT (Fig. 3). And then it decreases with time because the field-aligned plasma pressure gradient at the pole-ward edges of the depletions produces an equator ward force that drives plasma particles to move toward the equator (Le et al., 2003). Therefore nocturnal probability of occurrence of EPB is limited to the period 19:30 to 02:30 LT. The EPBs occur more frequently around midnight during low solar activity (Pimenta et al., 2001b). During periods of equinoxes (October, March and April) and solstice (November–February) the percentage of occurrence of EPBs increases gradually after sunset, reaches its maximum around 22:00 and 23:00 LT, respectively and then decreases gradually during high solar activity. According to Pimenta et al. (2001b), percentage of occurrence maximizes around 23:00 LT during November–February and then decreases gradually during high solar activity. Composition, neutral winds and strength of the equatorial plasma fountain effect play important role in seasonal occurrence of EPB at low latitude regions. If the fountain effect is more dominant, the northern equatorial ionization anomaly crest forms in pole-ward region with more plasma accumulated there (Lin et al., 2007).

4. Conclusion

We have analyzed all sky images, obtained at low-latitude station in Kolhapur in OI 630.0 nm, to study the occurrence characteristics of EPBs during period of high sunspot years (2010–11 and 2011–12). Herein we have concentrated on studies of nocturnal, seasonal and solar activity dependence on the occurrence of EPB. The principal features associated with these observations can be summarized as follows

(a) The nocturnal variation in occurrence of EPBs increases fairly rapidly after 19:30 LT and reaches a peak value at about 22:30 LT and then gradually decrease.
(b) The observed seasonal pattern of EPBs shows nearly no occurrence during May month and maximizes during the period October–April. The present results are very similar to that of Sahai et al. (1994, 1998).

(c) The equinox and solstice seasonal variations in the occurrence of EPBs show nearly equal and large differences respectively, during years of 2010–11 and 2011–12.
(d) The EPBs observed in equinox season during high sunspot year (2011–12) are possibly associated with solar activities (F 10.7 cm and >10 MeV proton flux) at low latitude station Kolhapur.

Equatorial spread-F has been studied for many years, but its understanding remains incomplete despite considerable progress. This paper contains empirical evidence of EPBs during high solar activity and these results are important for understanding the onset and growth conditions. Also, nocturnal and seasonal occurrences of EPBs are presented and these results are important in the ionospheric model.

Acknowledgements

One of the authors Mr. D. P. Nade is thankful to DST-PURSE for research assistantship. The nightglow observations at Kolhapur were carried out under scientific collaboration between Shivaji University, Kolhapur and Indian Institute of Geomagnetism (I.I.G.), Navi Mumbai. We also are thankful to the NOAA-GOES team for providing the solar and geomagnetic data over the Internet. One of the authors Mr. D. P. Nade is also thankful to Mr. R. B. Mane Sir (J. B. Patil High School Chipari, Kolhapur) and Miss R. P. Pawar (Department of Physics, Shivaji University, Kolhapur) for useful discussion on generation of plasma bubble.

We are thankful to Reviewers of this manuscript for given important comments.

References

Abalde, J.R., Fagundes, P.R., Sahai, Y., Pillat, V.G., Pimenta, A.A., Bittencourt, J.A. Height-resolved ionospheric drifts at low latitudes from simultaneous OI777.4 nm and OI630.0 nm imaging observations. J. Geophys. Res. 109, A11308, http://dx.doi.org/10.1029/2004JA010560, 2004.

Abdu, M.A., Sobral, J.H.A., Nelson, O.R., Batista, I.S. Solar cycle related range type spread-F occurrence characteristics over equatorial and low latitude station in Brazil. J. Atmos. Terr. Phys. 47, 901–905, 1985.

Chakraborty, S.K., DasGupta, A., Ray, S., Banerjee, S. Long-term observation of VHF scintillation and total electron content near the crest of the equatorial anomaly in the Indian longitude zone. Radio Sci. 34, 241–255, http://dx.doi.org/10.1029/98RS02576, 1999.

Chandra, H., Sharma, S., Abdu, M.A., Batista, I.S. Spread-F at anomaly crest regions in the Indian and American longitudes. Adv. Space Res. 31, 717–727, http://dx.doi.org/10.1016/S0273-1177(03)00034-6, 2003.

Chapagain, N.P., Fejer, B.G., Chau, J.L. Climatology of postsunset equatorial spread F over Jicamarca. J. Geophys. Res. 114, A07307, http://dx.doi.org/10.1029/2008JA013911, 2009.

DasGupta, A., Maritra, A., Basu, S. Occurrence of nighttime VHF scintillations near the equatorial anomaly crest in the Indian sector. Radio Sci. 16, 1455–1458, http://dx.doi.org/10.1029/RS016i006p01455, 1981.

Dashora, N., Taori, A., Patra, A.K. Multi instrument observation of winter solstice F-region irregularities during the low solar activity. Ind. J. Radio Space Phys. 41, 220–232, 2012.

Fagundes, P.R., Sahai, Y., Batista, I.S., Abdu, M.A., Bittencourt, J.A., Takahashi, H. Observations of day-to-day variability in precursor signatures to equatorial F-region plasma depletions. Ann. Geophys. 17, 1053–1063, 1999.

Huang, C.-M. Fregion irregularities that cause scintillations and spread-F echoes at low-latitude. J. Geophys. Res. 75, 4833–4841, http://dx.doi.org/10.1029/JA075i025p04833, 1970.

Jagtap, U.S., Sharma, A.K., Patil, P.T. Signature of plasma depletions using OI630.0 nm nightglow observations from 170°N latitude. Asian J. Chem. Environ. Res. 3, 70–73, 2010.

Jagtap, U.S., Sharma, A.K. OI 630 nm nightglow observations from Kolhapur (GEOG. LAT., 16.80 N; LONG.74.20 E) using tilting photometers during the magnetically quiet and disturbed nights. Asian J. Chem. Environ. Res. 1 (2–3), 15–21, 2008.

Kelley, M.C., Makela, J.J., de La Beaujardière, O., Retterer, J. Convective ionospheric storms: a review. Rev. Geophys. 49, RG2003, http://dx.doi.org/10.1029/2010RG000340, 2011.

Kelley, M.C. The Earth's Ionosphere. International Geophysical Services, vol. 43. Academic, San Diego, CA, 1989.

Kelley, M.C., Garcia, F., Makela, J., Fan, T., Mak, E., Sai, C., Alcocer, D. Highly structured tropical airglow and TEC signature during strong geomagnetic activity. Geophys. Res. Lett. 27, 465–468, 2000.

Le, G., Huang, C.-S., Pfaff, R.F., Su, S.-Y., Yeh, H.-C., Heelis, R.A., Rich, F.J., Hairston, M. Plasma density enhancements associated with equatorial spread F: ROCSAT-1 and DMSP observations. J. Geophys. Res. 108 (A8), 1318, http://dx.doi.org/10.1029/2002JA009592, 2003.

Lee, C.C., Chu, F.D., Chen, W.S., Liu, J.Y., Su, S.-Y., Liou, Y.A., Yu, S.B. Spread F, GPS phase fluctuations, and plasma bubbles near the crest of equatorial ionization anomaly during solar maximum. J. Geophys. Res. 114, A08302, http://dx.doi.org/10.1029/2009JA014195, 2009.

Lin, C.H., Liu, J.Y., Fang, T.W., Chang, P.Y., Tsai, H.F., Chen, C.H., Hsiao, C.C. Motions of the equatorial ionization anomaly crests imaged by FORMOSAT-3/COSMIC. Geophys. Res. Lett. 34, L19101, http://dx.doi.org/10.1029/2007GL030741, 2007.

Mukherjee, G.K., Carlo, L., Mahajan, S.H., Patil, P.T. First results of all-sky imaging from India. Earth Planets Space 50, 119–127, 1998.

Mukherjee, G.K., Carlo, L., Mahajan, S.H. 630 nm nightglow observations from 17°N latitude. Earth Planets Space 52, 105–110, 2000.

Mukherjee, G.K. Airglow and other F-layer variations in the Indian sector during the geomagnetic storm of February 5–7, 2000. Earth Planets Space 58, 623–632, 2006.

Mukherjee, G.K., Shetti, D.J. Plasma drift motion in F-region of ionosphere using photometric nightglow measurements. Ind. J. Radio Space Phys. 37, 249–257, 2008.

Nade, D.P., Sharma, A.K., Nikte, S.S., Ghodpage, R.N., Patil, P.T., Rokade, M.V., Vhatkar, R.S. Occurrence of F-region plasma bubble over low latitude station: Kolhapur, in: Proceedings of CARCAN-2012, Hyderabad, 21–22 December, pp. 94–99, 2012 (ISBN: 978-93-82570-04-2).

Parihar, N., Kakad, B.A., Mukherjee, G.K. Nightglow observations of OI 630 nm emission during the beginning of solar cycle 24 over 25°N. Ind. J. Radio Space Phys. 41, 155–161, 2012.

Pimenta, A.A., Fagundes, P.R., Bittewncourt, J.A., Sahai, Y. Relevant aspect of quatorial plasma bubbles under different solar activity conditions. Adv. Space Res. 27, 1213–1218, 2001a.

Pimenta, A.A., Fagundes, P.R., Bittencourt, J.A., Sahai, Y., Gobbi, D., Medeiros, A.F., Taylor, M.J., Takahashi, H. Ionospheric plasma bubble zonal drift: a methodology using OI 630 nm all-sky imaging systems. Adv. Space Res. 27, 1219–1224, 2001b.

Pimenta, A.A., Amorim, D.C.M., Candido, C.M.N. Thermospheric dark band structures at low latitudes in the Southern Hemisphere under different solar activity conditions: a study using OI 630 nm emission all-sky images. Geophys. Res. Lett. 35, L16103, http://dx.doi.org/10.1029/2008GL034904, 2008, 2008.

Sahai, Y., Aarons, J., Mendillo, M., Baumgardner, J., Bittencourt, J.A., Takahashi, H. OI 630 nm imaging observations of equatorial plasma depletions at 16°S dip latitude. J. Atmos. Terr. Phys. 56, 1461–1475, 1994.

Sahai, Y., Fagundes, P.R., Bittencourt, J.A., Abdu, M.A. Occurrence of large scale equatorial F-region plasma depletions during geo-magnetic disturbances. J. Atmos. Terr. Phys. 60, 1593–1604, 1998.

Sahai, Y., Fagundes, P.R., Bittencourt, J.A. Solar cycle effects on large scale equatorial F-region plasma depletions. Adv. Space Res. 24 (I I), 1477–1480, 1999.

Sahai, Y., Fagundes, P.R., Abalde, J.R., Pimenta, A.A., Bittencourt, J.A., Otsuka, Y., Rios, V.H. Transequatorial F-region ionospheric plasma bubbles: solar cycle effects. J. Atmos. Terr. Phys. 62, 1377–1383, 2000.

Sahai, Y., Fagundes, P.R., Becker-Guedes, F., Abalde, J.R., Crowley, G., Pi, X., Igarashi, K., Amarante, G.M., Pimenta, A.A., Bittencourt, J.A. Longitudinal difference observed in the ionospheric F-region during the major geomagnetic storm of 31 March 2001. Ann. Geophys. 22 (9), 3221–3229, 2004a.

Sahai, Y., Fagundes, P.R., Abalde, J.R., Pimenta, A.A., Bittencourt, J.A., Otsuka, Y., Rios, V.H. Generation of large-scale equatorial F-region plasma depletions during low range spread-F season. Ann. Geophys. 22, 15–23, 2004b.

Scherliess, L., Fejer, B.G. Storm time dependence of equatorial disturbance dynamo zonal electric fields. J. Geophys. Res. 102, 24037–24046, 1997.

Sharma, A.K., Nade, D.P., Nikte, S.S., Ghodpage, R.N., Patil, P.T., Rokade, M.V., Vhatkar, R.S. Analysis of plasma bubbles observed in night airglow emission line OI 630.0 nm from Kolhapur using all sky imager. Int. J. Eng. Sci. Res. 3 (2), 746–750, 2012.

Sharma, A.K., Nade, D.P., Nikte, S.S., Ghodpage, R.N., Patil, P.T., Rokade, M.V., Vhatkar, R.S., Gurubaran, S. Development of fast image analysis technique for all sky images. Curr. Sci., Manuscript ID 575, accepted for publication.

Shvarts, D., Alon, U., Ofer, D., McCrory, R.L., Verdon, C.P. Nonlinear evolution of multi-mode Rayleigh–Taylor instability in two and three dimensions, in: Proceedings of the Fifth International Workshop on Compressible Turbulent Mixing. World Scientific (ISBN: 9810229100), 1996.

Sinha, H.S.S., Rajesh, P.K., Misra, R.N., Dutt, N. Multi-wavelength imaging observations of plasma depletions over Kavalur, India. Ann. Geophys. 19, 1119–1131, 2001.

Taori, A., Makela, J.J., Taylor, M. Mesospheric wave signatures and equatorial plasma bubbles: a case study. J. Geophys. Res., http://dx.doi.org/10.1029/2009JA015088, 2010.

Taori, A., Patra, A.K., Joshi, L.M. Gravity wave seeding of equatorial plasma bubbles: an investigation with simultaneous F-region, E-region and middle atmospheric measurements. J. Geophys. Res. 116, http://dx.doi.org/10.1029/2010JA016229, 2011.

Taori, A., Kamalakar, V., Joshi, L.M., Sripathi, S., Patra, A.K. On the linkage between mesospheric gravity waves and occurrence of equatorial plasma bubble observed during the low solar activity. Ind. J. Radio Space Phys. 41, 264–270, 2012.

Taori, A., Jayaraman, A., Kamalakar, V. Imaging of mesosphere–thermosphere airglow emissions over Gadanki (13.5°N, 79.2°E) first results. J. Atmos. Terr. Phys. 93, 21–28, 2013.

Taylor, M.J. A review of advances in imaging techniques for measuring short period gravity waves in the mesosphere and lower thermosphere. Adv. Space Res 19, 7–616, 1997.

Weber, E.J., Buchau, J., Eather, R.H., Mende, S.B. North–south aligned equatorial airglow depletions. J. Geophys. Res. 83, 712–716, 1978.

Weber, E.J., Buchau, J., Moore, J.G. Airborne studies of equatorial F-layer ionospheric irregularities. J. Geophys. Res. 85, 4631–4641, 1980.

Whalen, J.A. Dependence of equatorial bubbles and bottom side spread F on season, magnetic activity and $E \times B$ drift velocity during solar maximum. J. Geophys. Res. 107, http://dx.doi.org/10.1029/2001JA000039, 2002.